Contents

As separate files:

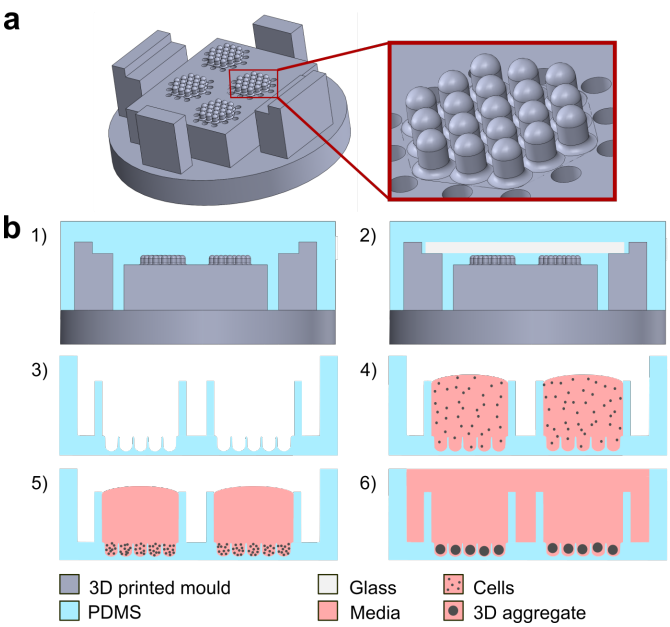

Supplementary Fig. 1 | Design, production, and use of the micro-well duct-on-chip technology. a, 3D printed micro-well chip mould of a 600 μm well diameter. **b,** Schematic of the micro-well chip fabrication (steps 1–3) and cell seeding process (steps 4–6). Step 1: PDMS is poured into the 3D printed mould. Step 2: A glass slide is aligned to imprinted spacers of the mould. Step 3: PDMS is released from the mould and glass. Step 4: After passivation of PDMS with the hydrophobic co-block polymer pluronic-F127, cells resuspended in 20–40 μL of media are pipetted into the micro-well arrays held by surface tension due to the 12 surrounding pillars. Step 5: Cells settle into the micro-wells within 30 min. Step 6: The micro-well chip is filled up to 800 μL of media and cells aggregate within 4 h.

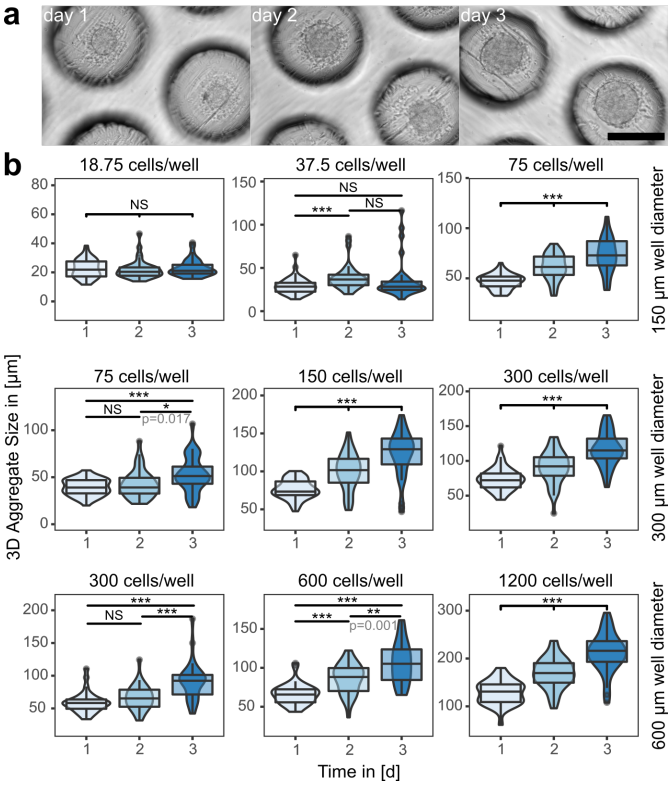

Supplementary Fig. 2 l Size and growth of hiPSC 3D aggregates grown in the micro-wells over 72 h. a, Representative bright-field images of 3D hiPSC aggregates from initial 150 cells per well 24, 48, and 72 hours after seeding on the micro-well chip. Scale bar is 200 μm. **b,** Size distribution of hiPSC derived 3D aggregates 24, 48, and 72 h after seeding in wells with a diameter of 150, 300, and 600 μm (from top to bottom). The number of cells seeded per well was systematically varied to optimize the growth and viability of the 3D aggregates. Per condition, 52 3D aggregates were measured from three different micro-well arrays. Boxplots display the median with the first and third quartile, whiskers denote the 1.5x interquartile range and outliers are marked as dots. Significance levels are indicated as follows: *: p-value<0.05; **: p-value< 0.01; ***: p-value<0.001 and calculated with a two-sample Welch test.

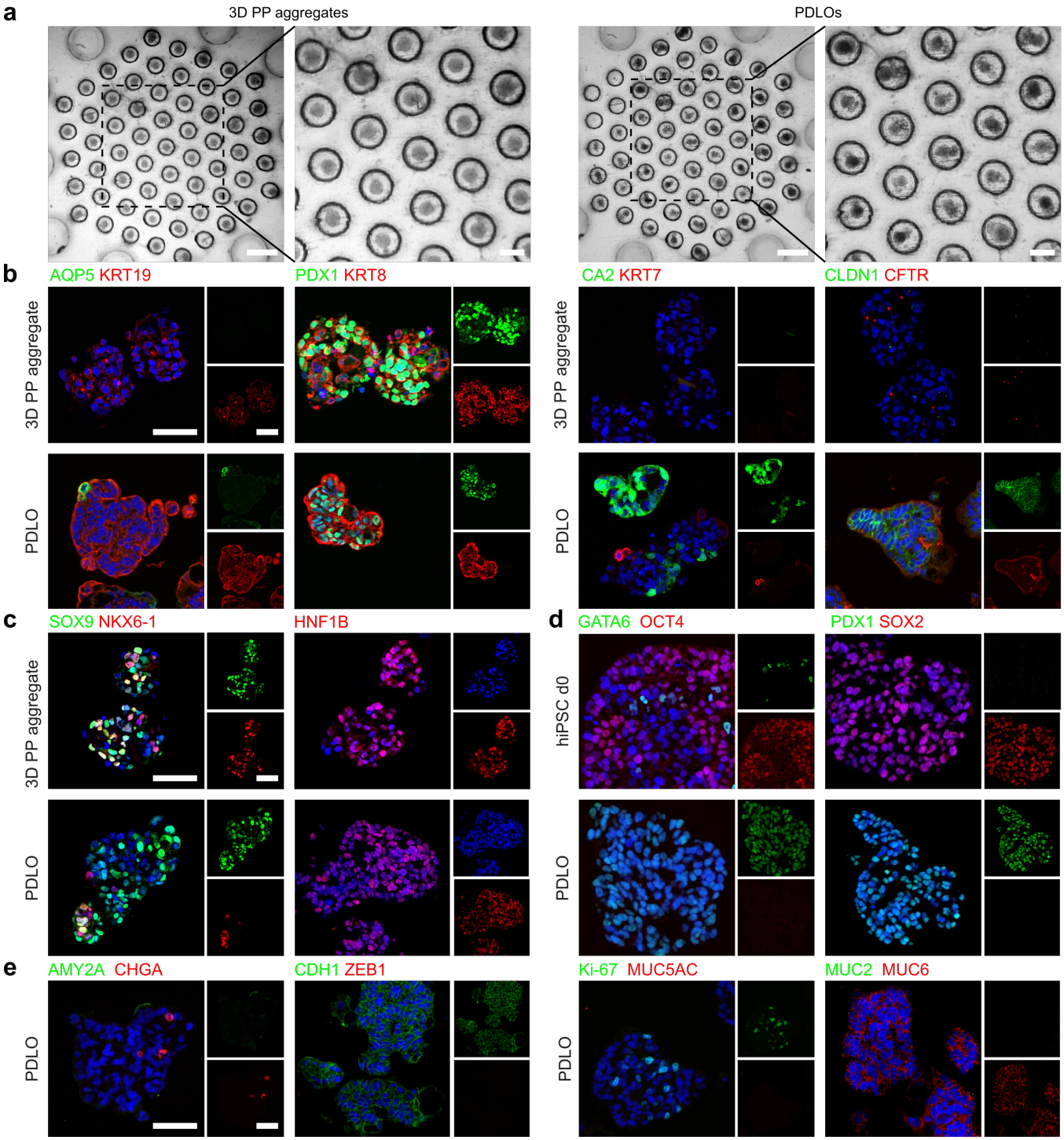

Supplementary Fig. 3 | Characterization of PDLOs (day 28) on the micro-well chip. a, Overview bright-field image of one micro-well chip array of 3D PP aggregates on day 14 and of the same array on day 27 of differentiation (representative images for five independently started differentiations). Scale bares denote 500 μm and 200 μm for the zoom-in. **b-e,** 3D PP aggregates on day 14 of differentiation are depicted as controls. Fluorescence images of the 3D PP aggregates and PDLOs to confirm pancreatic ductal identity. All scale bars: 50 μm. **b**, Pancreatic ductal proteins. **c**, Reduction of endocrine PP marker NKX6-1, while expression of ductal PP marker HNF1B was maintained. **d**, Stem cell marker OCT4 and stem cell and anterior foregut marker SOX2 expression were lost in PDLOs. **e**, While no signs for acinar cells (AMY2A) were found, a small subset of cells expressed endocrine markers such as CHGA. Homogenous expression of epithelial cell marker CDH1 was observed, but not the mesenchymal marker ZEB1. Few cells expressed the proliferation marker Ki-67 at day 28 in PDLOs, whereas gastric and dysplasia marker MUC5AC and intestinal marker MUC2 were absent. MUC6 expression indicative for pancreatic ducts was widely expressed in PDLOs.

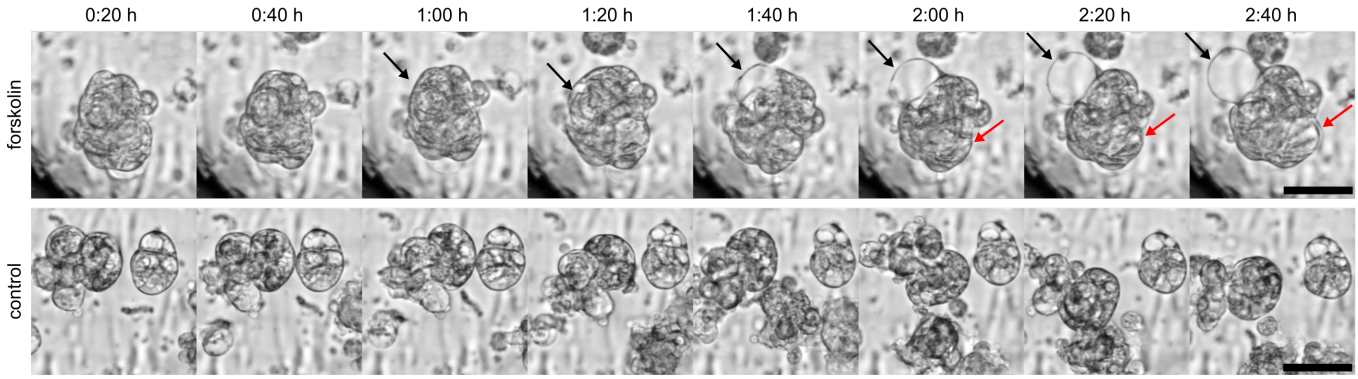

Supplementary Fig. 4 | Swelling of PDLOs upon stimulation with forskolin. Live imaging over the first 2 h and 40 min of stimulation with 20 μM forskolin and 100 μM IBMX; and control with H_2O. Scale bar denotes 50 μm.

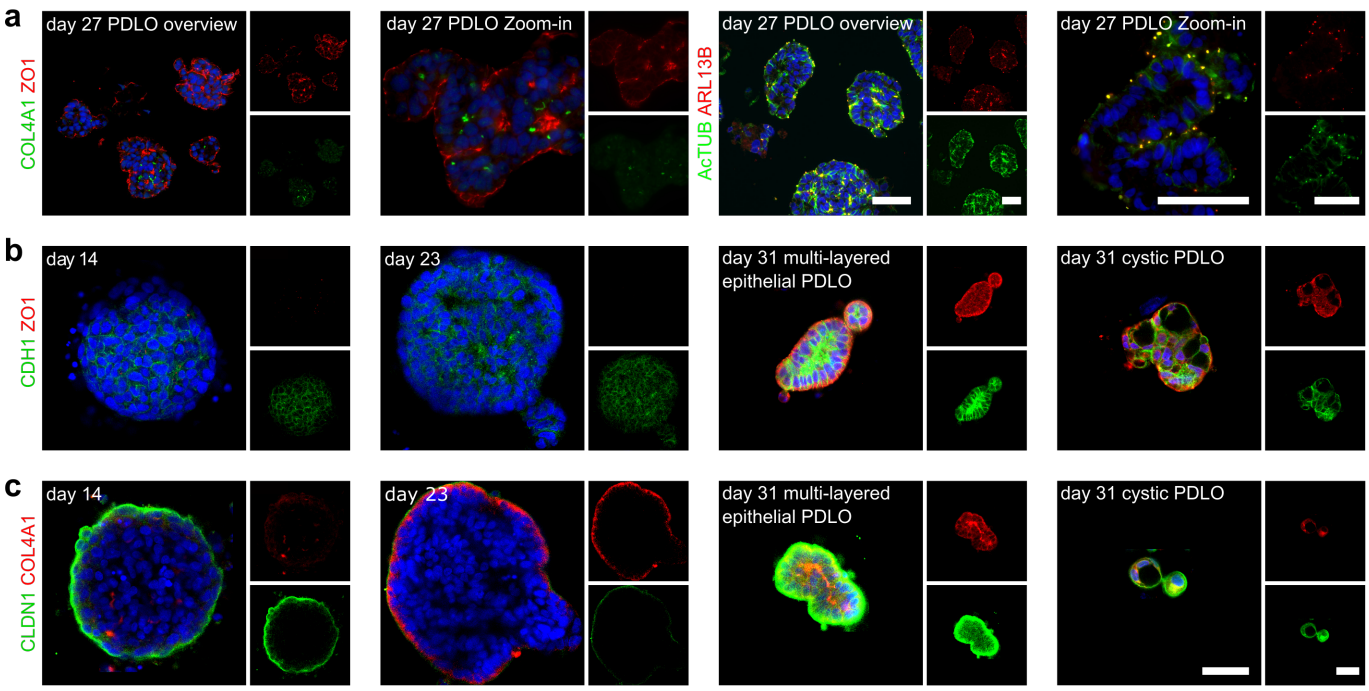

Supplementary Fig. 5 I Apical-outside polarity of PDLOs. a, Overview and magnification of apical-basal polarity images of PPs and PDLOs shown in Fig. 3d. **b** and **c**, Fluorescence images of polarity markers ZO1, CDH1 and COL4A1, CLDN1 over the time course of ductal differentiation.

a

Sample	Cell Number
Day 13	6705
Day 14	4436
Day 16	608
Day 20	505
Day 23	625
Day 27	488
Day 31(both samples)	1444

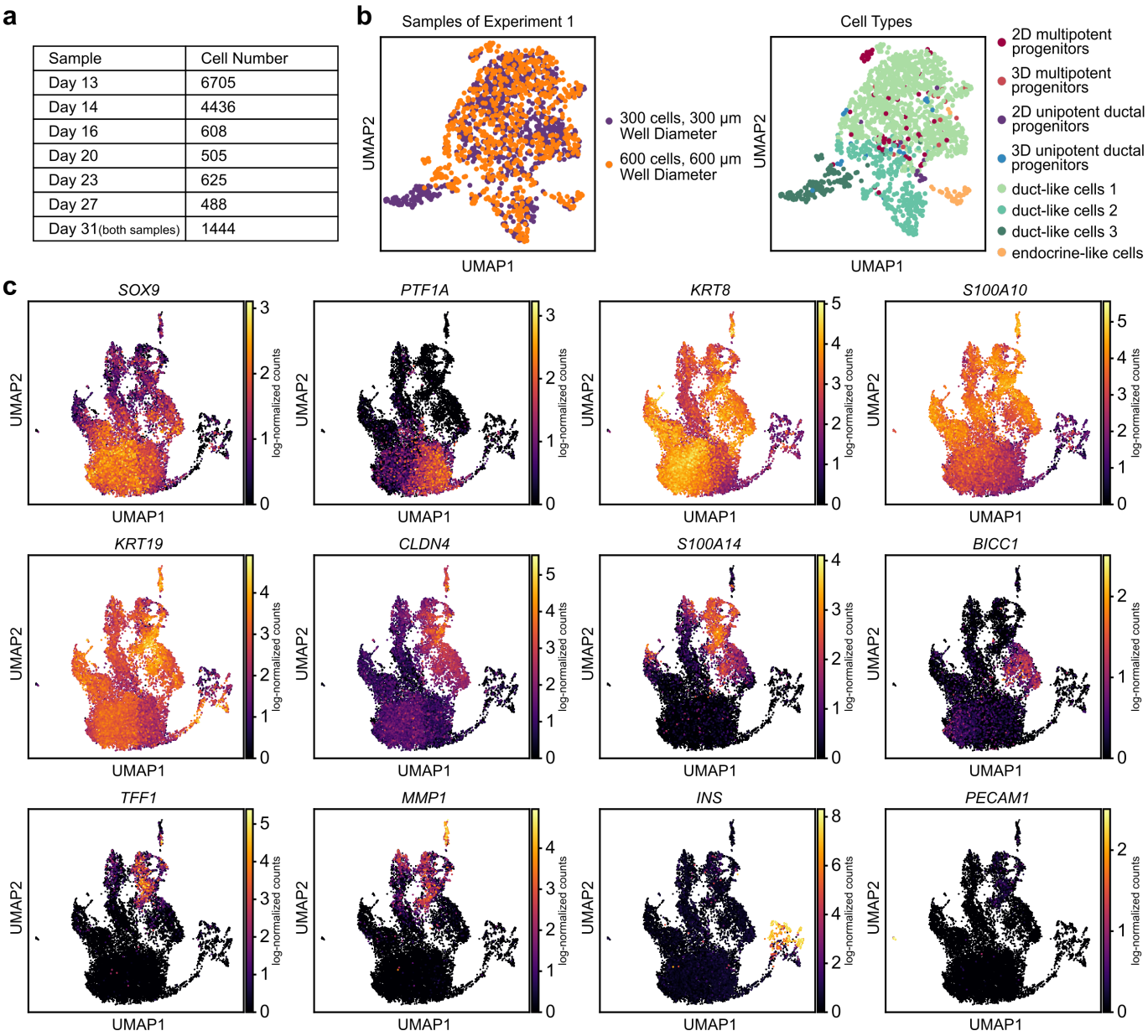

Supplementary Fig. 6 | Influence of the well diameter and seeded cell number per well on ductal differentiation determined by scRNA-seq. a, Single-cell count statistics for the cells presented in Fig. 3. **b,** UMAP cluster plot of single-cell transcriptomes acquired from PDLOs after 31 DOD. While in one condition, 3D aggregates were initiated with 300 cells per well in wells with a diameter of 300 μm, in the other condition, 3D aggregates were formed by 600 cells in a 600 μm well. In the second UMAP plot cell types from experiment 1 are assigned according to Fig. 3c. **c**, UMAP plots of the single-cell transcriptomes highlighting the cluster-specific expression of differentially regulated pancreatic progenitor and ductal markers. Complementary to Fig. 4e.

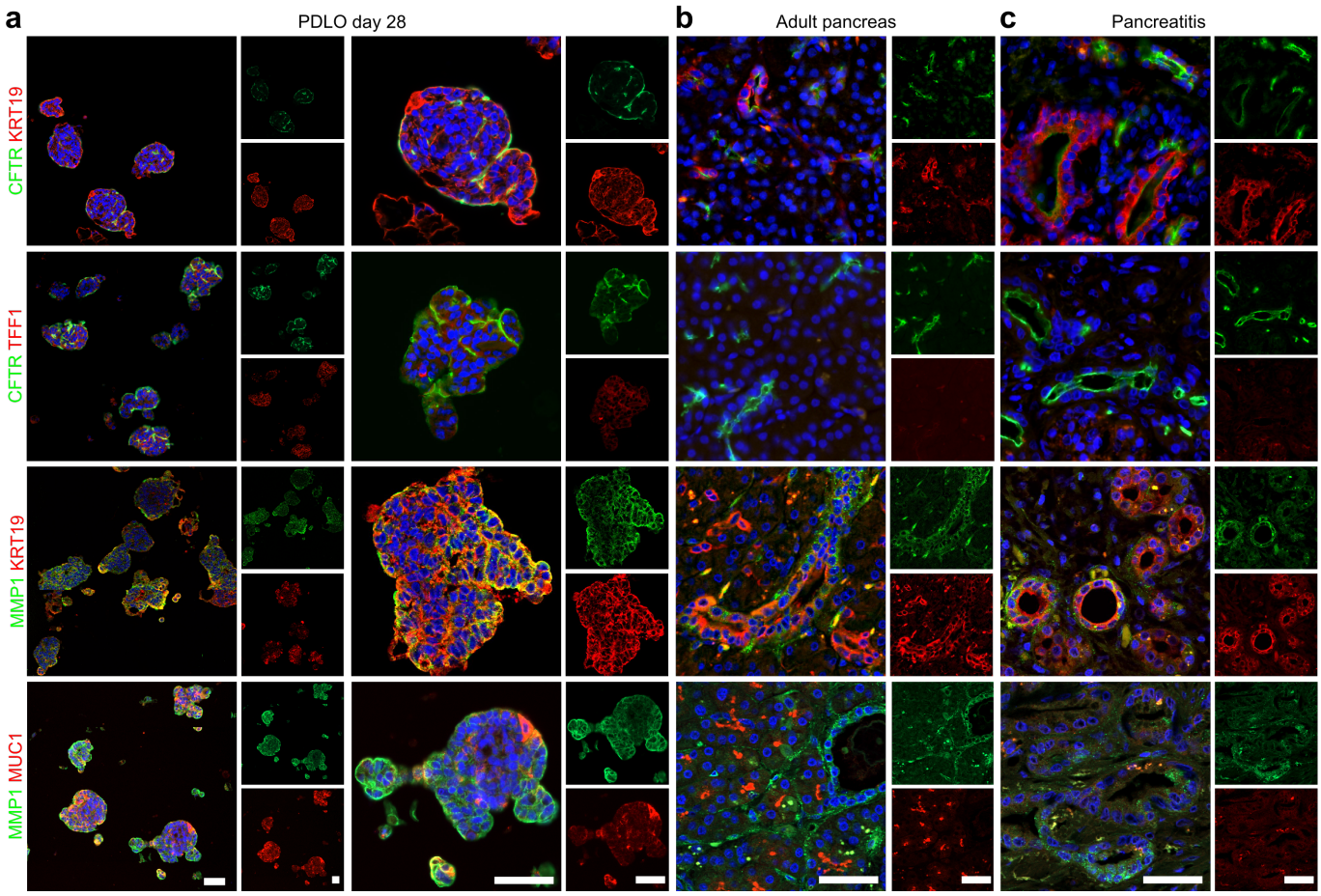

Supplementary Fig. 7 | Ductal subcluster-specific genes located within PLDOs and primary pancreas tissue on the protein level. a, PDLOs differentiated until day 28 stained for cell subtype markers and pan-ductal marker KRT19. **b**,**c**, The same markers are used to locate the *in vitro* generated ductal-like cell subtypes in healthy human primary pancreas tissue and tissue from pancreatitis patient, respectively. Images are complementary to Fig. 5. Scale bar denotes 50 μm.

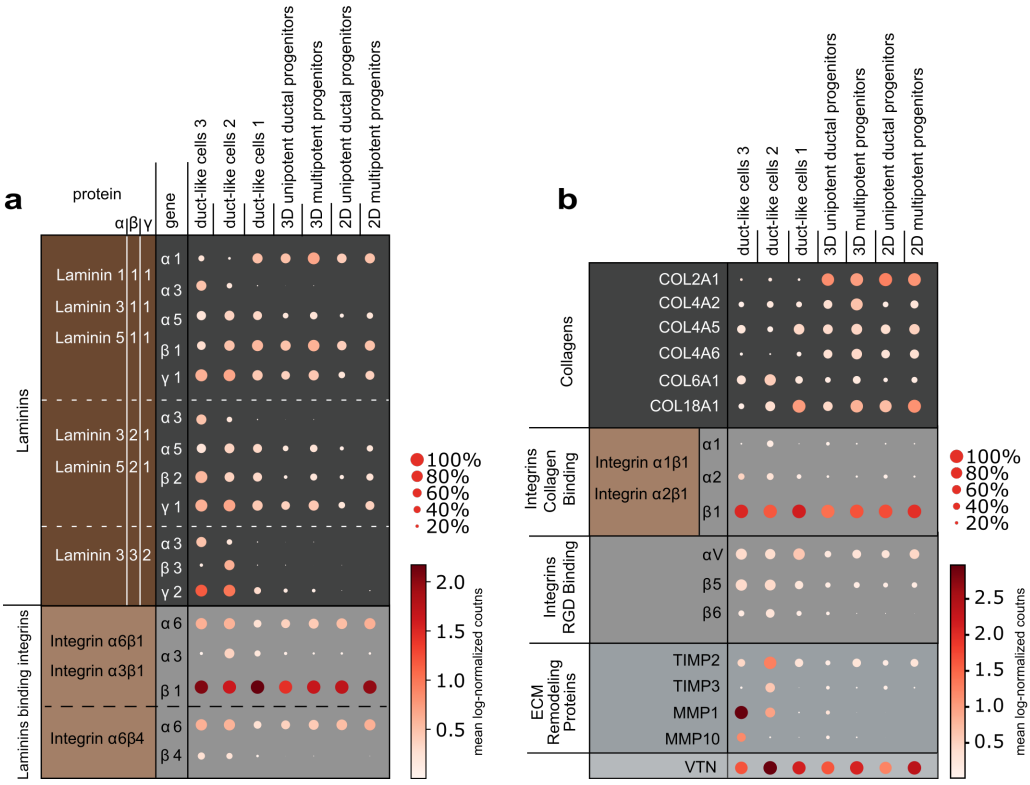

Supplementary Fig. 8 | Single-cell transcript analysis of genes associated with extracellular matrix (ECM) showing dynamical expression during the differentiation trajectory of PDLOs. Dynamical genes were determined by the velocity analysis in main Fig. 5. **a,** Dot plot shows the change of laminin and laminin-binding integrin gene expression within the cells of the different clusters. **b**, Dot plot shows the change of collagen, collagen-binding integrins, and ECM remodelling gene expression within the cells of the different cluster during differentiation.

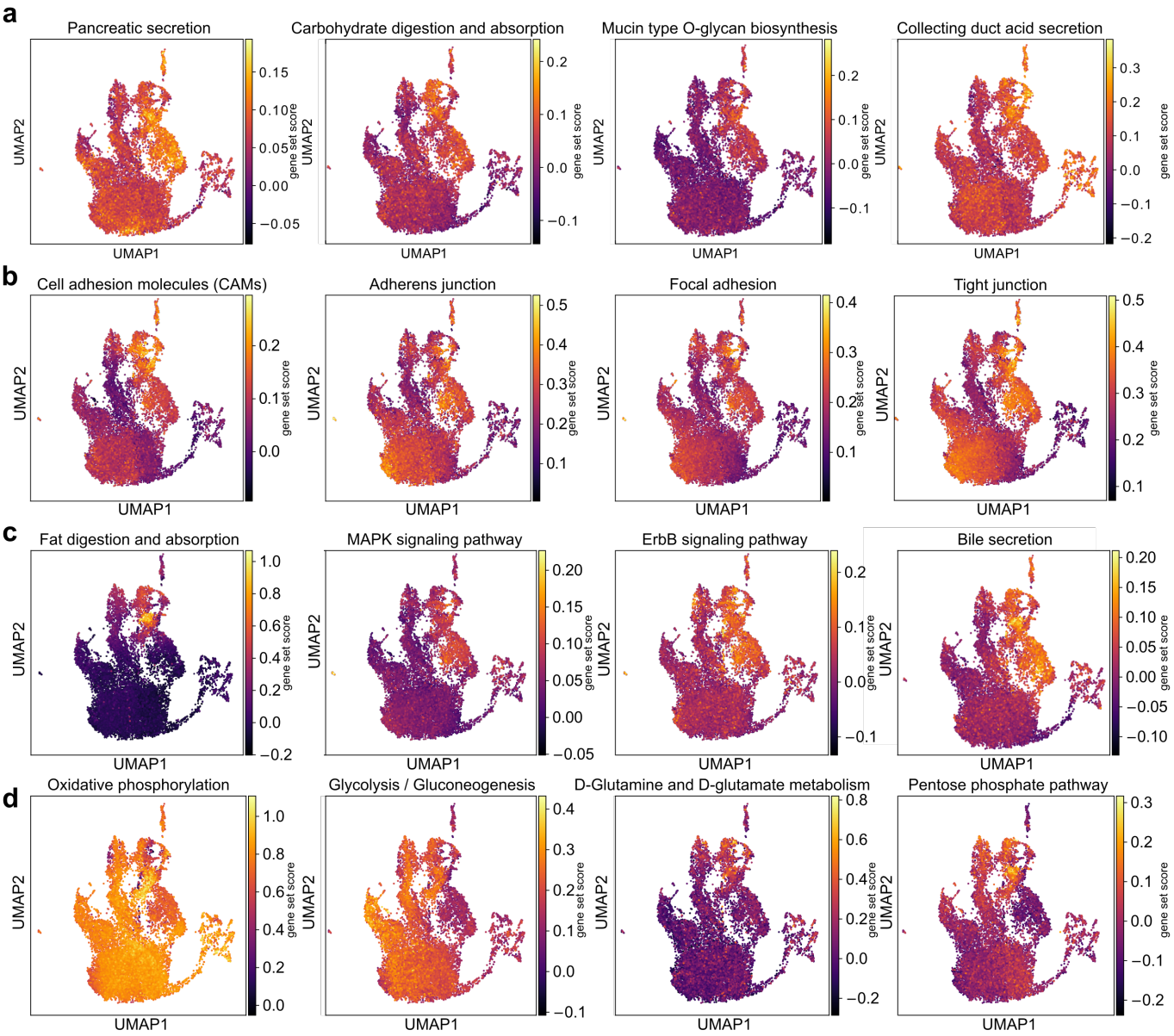

Supplementary Fig. 9 | Pathway enrichments within the ductal transcriptional differentiation kinetics with focus on a, ductal function, **b,** epithelial cell organization, **c,** pancreas function and signalling, and **d,** metabolic energy conversion.

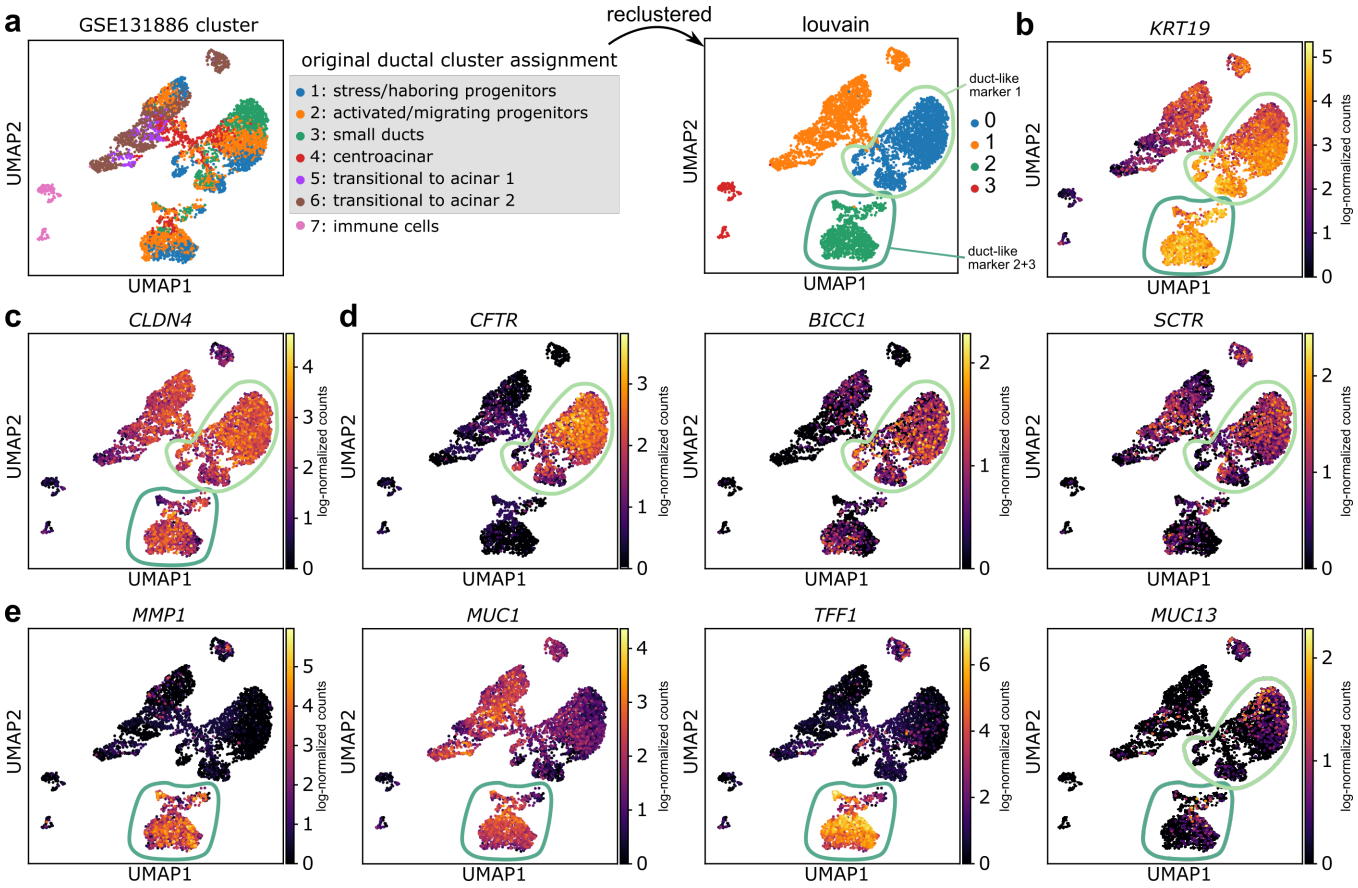

Supplementary Fig. 10 | CFTR+ and mucin-rich duct-like cell type markers map cell populations derived from primary human pancreas[26]. **a**, Reanalysis of primary human ductal scRNA-seq data[26]. **b** and **c**, *KRT19* and *CLDN4* marker mapped on the cell data set. **d**, Expression patterns of ductal-like marker genes for the three subpopulations derived from PDLOs. *CFTR/BICC1/SCTR* and *MMP1/MUC1/TFF1* positive cells (colour coded circles) separate in the data set, whereas *MUC13* shows an overlap between the ductal cell clusters in the primary data.

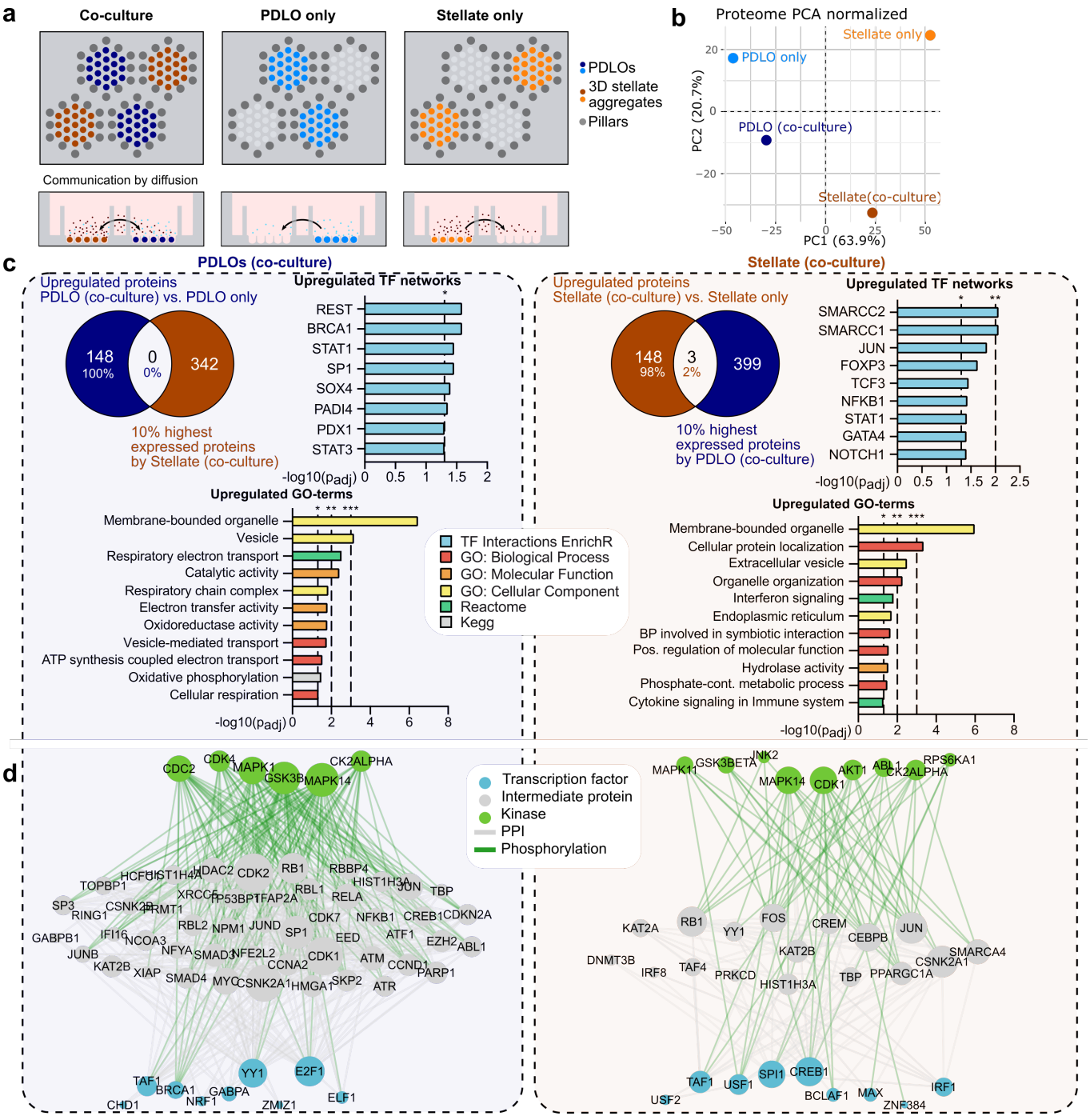

Supplementary Fig. 11 | Co-culturing of PDLOs and human pancreatic stellate cell (HPaSteC) aggregates on a micro-well chip. a, Micro-well chip experiment for co-culturing PDLOs and 3D HPaSteC aggregates. The four fluidically separable hexagonal arrays on the micro-well chip enabled co-cultures of PDLOs and HPaSteCs without mixing cell types. After 3 days of co-culture, the proteomes of both cell types were determined by label-free mass spectrometry. **b**, Principal component analysis (PCA) separating co-culture of PDLOs and HPaSteCs from their individual cultures (n=1). **c**, Cross-contamination test and GO term analysis of the upregulated protein sets in PDLOs and HPaSteCs. Protein interactions with several transcription factors such as STAT1, STAT3 or JUN, STAT1, NFKB were enriched and GO terms indicated an increased autocrine and paracrine signalling (membrane-bounded organelle, extracellular vesicle, vesicle-mediated transport) and energy consumption (respiratory electron transport, respiratory chain complex, ATP synthesis, or oxidative phosphorylation). Significance levels are indicated as follows: *: p-value<0.05; **: p-value< 0.01; ***: p-value<0.001. **d**, Protein network analysis[93] of the upregulated protein sets in co-cultured PDLOs and HPaSteCs suggested reciprocal signalling. In both cell types, we found mitogenic signalling, enabled by the diffusion-driven communication of the co-cultured cells.

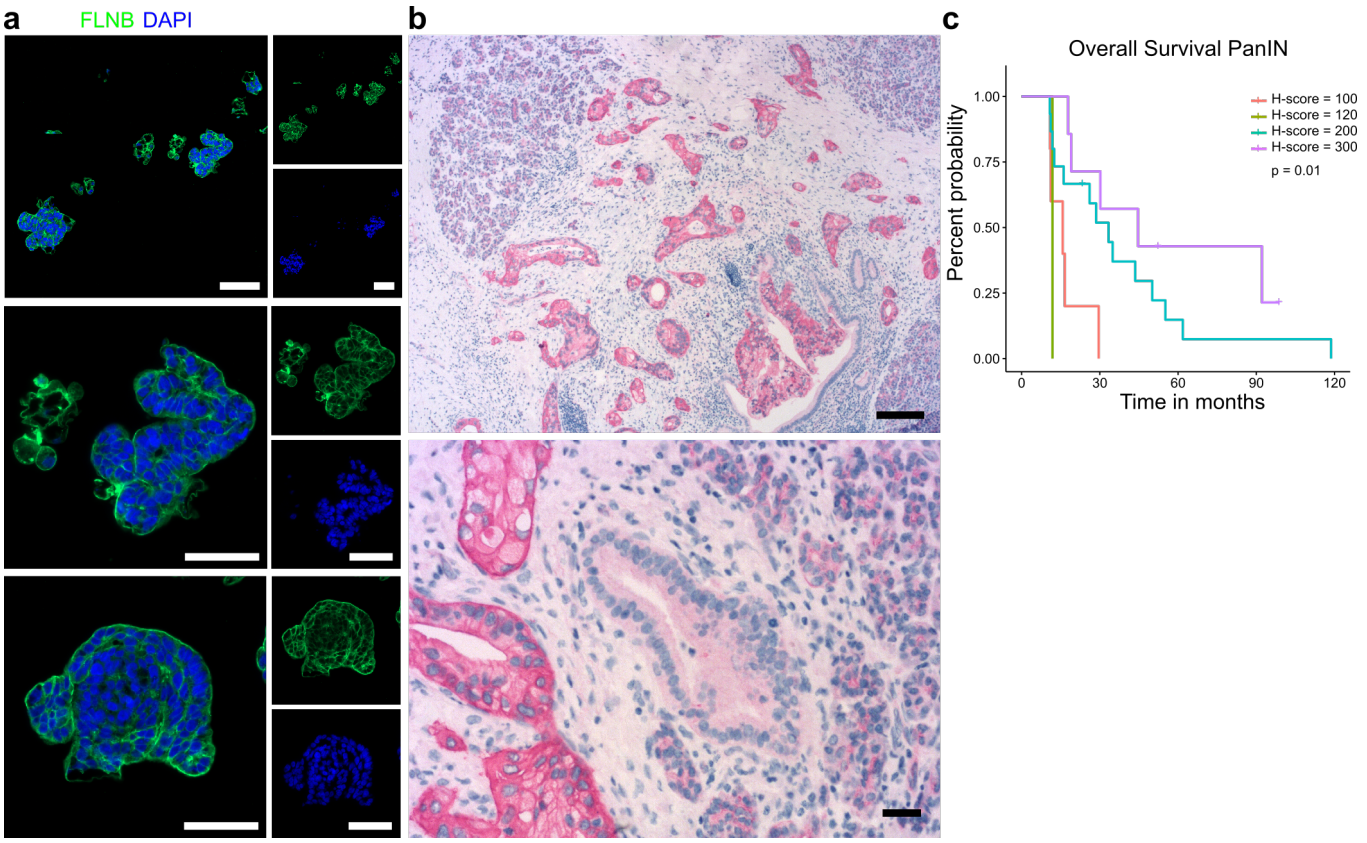

Supplementary Fig. 12 | FLNB expression in PDLOs and PDAC and overall survival curve of FLNB. a, Fluorescence images of PDLOs stained for FLNB. Scale bar denotes 100 μm (overview) and 50 μm (magnifications). **b**, Different image magnifications of FLNB IHC staining of PDAC tissue related to Fig. 8e. Scale bars denote 100 μm (overview) and 20 μm (magnification). **c**, Computationally generated Kaplan Meyer plot for FLNB. P-value was calculated with the log-rank test.